Evolutionary stability of social commitment

Yuka Shirokawa [a, *], Masakazu Shimada [a], Nao Shimada [a], Satoshi Sawai [a, b]
[a] Graduate School of Arts and Sciences, University of Tokyo, Tokyo 153-8902, Japan;
[b] Research Center for Complex Systems Biology, University of Tokyo, Tokyo 153-8902, Japan;

* To whom correspondence should be addressed: Yuka Shirokawa
Email: shirokawa.yuka@gmail.com

Author Contributions: Y.S., M.S., and S.S. designed the research; Y.S. initiated and performed all aspects of the research including data and model analysis; Y.S., N.S., and S.S. contributed new reagents; Y.S., and S.S. wrote the paper.

Keywords: Cooperation; physiological irreversibility; valley of fitness landscape; division of labor; developmental stability; multicellularity

Abstract

Conflict resolution between individual cells and a group is essential for multicellularity. The social amoeba *Dictyostelium discoideum* switches between solitary growth and social fruitification depending on nutrient availability. Under starvation, cells form fruiting bodies consisting of spores and non-viable altruistic stalk cells. Once cells socially committed, they complete fruitification even with a renewed source of nutrients. This social commitment is puzzling because it deprives individual cells of benefits of quickly resuming solitary growth. One idea posits that traits that facilitate premature de-commitment are somehow hindered from being selected. We studied outcomes of premature de-commitment by forced refeeding. We show that when refed cells resume sociality together with non-refed cells, besides some becoming solitary outside of fruiting bodies, a large fraction was redirected to a sub-region of altruistic stalk regardless of their original fate. The refed cells exhibited reduced cohesivity and were sorted out to the altruistic positions in morphogenesis. Furthermore, a theoretical model considering evolution of cell-cell association revealed a valley in the fitness landscape that prevents invasion of de-committing mutants. Our results provide a general scheme that naturally penalizes withdrawal from a society by evolving a specific division of labor that less cohesive individuals become altruists.

Significance Statement

Evolution of unicellular to multicellular organisms must resolve conflicts of reproductive interests between individual cells and the group. In the social amoeba *Dictyostelium*, a transition from a solitary to multicellular group occurs under starvation. Once cells commit themselves to multicellular organization, the process continues even when shifting to an environment that favors solitary growth. Our study revealed that cells forced to partially revert to a de-committed state take an altruistic role through interaction with socially committed cells. The de-committed cells exhibited reduced cohesivity and were sorted out to altruistic positions in morphogenesis. This inevitably penalizes 'selfish' cells that revert to solitary growth too quickly. Our results explain group-level behavior that is apparently difficult to understand from an individual-level fitness.

Main Text

Introduction

Cohesion of a group is fundamental to making cooperation fruitful for group members. However, evolution of cooperation is often faced with selection pressures that potentially lead to their collapse. Cheating that exploits benefit of cooperation at the cost of others is a well-studied case of such risks. Nature has found ways to reduce deleterious effects of cheating through interactions among kin [1] and policing that suppress individual proliferation [2]. In microbial cooperation [3], colony expansion that keeps the cooperator cells at close distances [4, 5] and kin recognition using cell-surface proteins [6, 7] play pivotal roles in cheating suppression. Besides cheating, cooperation is also vulnerable to transient environmental changes that raise fitness of a cell as a solitary individual rather than as a social group member. Indeed, evolutionary loss of social behavior has been experimentally demonstrated in myxobacteria under conditions that impede their social interaction while favoring solitary reproduction [8]. Phylogenetic analyses have also shown that the social loss appears to be a common phenomenon across taxa from insects to unicellular organisms [9–11]. Social behavior exemplified by a high degree of division of labor and reproductive skew is thought to have crossed a 'point of no return' [12, 13] back to a solitary lifestyle due to its high complexity. The stabilization of cooperation against adverse evolutionary pressures is the key driving force that increases social complexity [14, 15].

How sociality is precluded from reverting to a free-living lifestyle is especially non-trivial in social groups consisting of individual cells that can survive on their own. One explanation is that social traits act disadvantageously for unicellular growth. For example, in the experimental evolution of fission yeast, high rates of apoptosis evolve to promote snowflake-like chains of cells with high nutrient availability. Since apoptosis is disadvantageous for solitary proliferation [14, 16], multicellularity should be maintained [14, 15]. However, such a trade-off may be limited to cases where individual cells can immediately escape the group. The example of the social loss in myxobacteria, which exhibits intermediate social behavior such as reduced sporulation and collective motility [8], hints at the importance of intermediate phenotypes in the evolutionary transition [17]. Given that even simple multicellularity is a multifactorial trait regulated by a large number of genes [18], loss of sociality almost inevitably proceeds through a transition stage where a newly emerging lineage exhibits the intermediate phenotype, meaning

that it still interacts with other socially committed cells. In this situation, the social loss may be prevented if the intermediate phenotypes are somehow hindered from being selected, but at least, a new costly countermeasure should not evolve because they are in an environment that favors solitary growth. One of the simplest ways is that the preexisting social defense itself comes with a rather unexpected bonus of acting inhibitory to reversion to a solitary lifestyle. To obtain the unexpected bonus, the defensive function should have incomplete target specificity. For example, social microbes evolve traits that suppress the sporulation of cheaters [19, 20], but how specific it is to a certain genotype is poorly explored. In other examples, bacteriocins spite cells that are sensitive to the signal in an indiscriminatory manner [21]. Given that such elimination of 'nonself' is a common and fundamental defense strategy in organisms [22], what may underlie defensive behavior are exclusion of deviators from the original members, which would inevitably suppress the intermediate phenotypes. Taken together, how the intermediate phenotypes between a social and solitary state interact with the original social members is critical in understanding the maintenance of social behavior.

The social amoeba *Dictyostelium discoideum* is a soil-living eukaryote with facultative sociality under non-nutrient conditions [23, 24]. The cells grow and divide in the presence of nutrient sources such as bacteria and fungi, however, when starved, they aggregate to form a multicellular slug that culminates in a fruiting body composed of differentiated spores and stalk cells. *Dictyostelium* has served as a model microorganism to study cellular cooperation [25], since death of stalk cells that support the spores [23, 24] can be viewed as altruistic behavior. Interestingly, after 4 to 6 hours of starvation onward, cells become engaged in the differentiation process [26], and will no longer quickly revert back to the growth phase even with renewed nutrient supply [27]. Instead, cells continue with the formation of fruiting bodies within 24 hours. The inability of differentiating cells to switch back to solitary growth (hereafter referred to as social commitment) is dependent on the multicellular context. When cells that are mechanically dissociated are replenished with nutrients, they revert to solitary growth [26–28]. Thus, unless mechanical dissociation, the only way by which cells return to the solitary state is to mature into spores and then germinate, a long process that takes a few days. Evolutionary benefit of the social commitment is puzzling, especially given that the social amoeba colonizes sites with a frequent supply of rich dung or leaf mold [29], which favor quick reversion to solitary growth. Existence of a phagocytic cell type that removes intruding bacteria within a slug [30] suggests that it is not unusual for socially committed cells to be exposed to nutrients. To understand the multicellular basis that maintains the social commitment in *Dictyostelium*, we studied outcomes of premature de-commitment. In our experiments, cells were forced to take the dedifferentiation path by short-term refeeding, and their fates when mixed with socially committed cells were traced by live-cell imaging. Based on the observation, a theoretical model was constructed to predict the evolutionary stability of the social commitment.

Results

Forced refeeding experiments

126 Mechanically dissociated cells re-plated on agar without nutrients are known to rapidly
127 reaggregate and recapitulate the respective developmental stages within a few hours [31]. We
128 exploited this unique property to investigate the interactions between socially committed and
129 partially de-committed cells. For the de-committed cells, dissociated cells from the slug stage
130 were fed with bacteria *Escherichia coli* B/r for 3 or 5 h (hereafter referred to as RF3 and RF5
131 cells, respectively), then nutrients were removed again. The refed cells were then allowed to
132 reaggregate with cells that were not refed (NF cells, socially committed cells) (Figure 1*A*). This
133 treatment mimics a situation that a rare cell makes a slug with socially committed cells and
134 dedifferentiates to engulfing bacteria within a slug, where the bacteria remained for 3 to 5 h
135 before the terminal differentiation (18 to 23 h after starvation). A strain harboring the prestalk
136 (ecmAO-RFP) and prespore (pspA-GFP) marker genes were used for identification of their
137 original cell fate owing to the time for degradation of fluorescent proteins (> 4–5 h) [32]. The
138 mixture of cells jointly formed a tight mound after 1.5–2 h (Figure S1, Movies S1 and S2). In the
139 mixture of NF cells with and without the cell-type reporter (NF+NF), prestalk cells were found in
140 the peripheral region of the aggregate, while prespore cells were more uniformly distributed
141 (Figure 1*B*: NF+NF) in line with the previously described sorting pattern [33]. In contrast, in the
142 mixture of RF and NF cells, RF cells (fluorescent cells) were positioned at the periphery
143 regardless of the original cell type (Figure 1*B*: RF3/5+NF), while NF cells (non-fluorescent cells)
144 were more abundant in the aggregation center. Thus, the refed treatment significantly affected
145 cell positioning (Figure 1*C,* Table S1: overall model: GLM and analysis of deviance, cell fate: $P <$
146 0.0001, treatments: $P < 0.0001$, prespore cells in NF+NF versus RF5+NF: *t*-test, adjusted $P <$
147 0.0001). In the swap control, we observed a consistent pattern (Figure S2*A*, RF(Fl-)+NF(Fl+)),
148 indicating that expression of the marker genes itself did not affect the sorting pattern.
149 Furthermore, our supporting data indicates that the segregation was relative behavior when RF
150 cells interact with the NF cells because RF cells were still fully capable of developing on their
151 own (Figure S2*B*), and the unique sorting pattern was not merely due to mechanical interruption
152 but also required nutrient replenishment (Figure S2*C*).
153 Quantitative real-time polymerase chain reaction analysis (real-time PCR, Table S2,
154 see *SI* Methods) showed that RF cells exhibited reduced expression of cell-type differentiation
155 marker genes (Figure 1*D*, *pspA*, *ecmA*), indicating partial dedifferentiation (Figure 1*D,* Table S1:
156 bootstrap test, adjusted $P > 0.025$). Whereas genes encoding the main adhesion molecules [34]
157 (*cadA*, *csaA*, and *tgrC1*) did not show nutrient-specific changes, *carA*, *acaA*, *pdsA,* and *dscA*
158 genes (Figure 1*D*) showed contrasting activity of being reduced by refeeding and induced in non-
159 nutrient buffer (Figure 1*D,* Table S1: GLM and analysis of deviance, 'No-nutrient' versus
160 'Bacteria': adjusted $P < 0.05$, 'No-nutrient' versus 'Growth medium': adjusted $P < 0.01$). *CarA*,
161 *acaA*, and *pdsA* are essential for the cAMP relay during cell aggregation, and *dscA* (discoidin I) is
162 implicated in the cell-substratum adhesion during aggregation [35, 36].
163 Given that RF cells show reduced expression of the re-aggregation genes, they are likely
164 to fall behind in joining cell clusters by delayed chemotaxis. However, RF cells appear well
165 mixed and then sorted out afterward (Figure S1, Movie S2). Although a recent work suggested a
166 sorting mechanism of a tip-forming prestalk subtype [37], RF cells are sorted to the periphery
167 and then to the base of the mound instead of the apical tip (Figure S3*A*). These observations
168 point to an alternative mechanism based on differential adhesion [38], where cell-type that

169 position themselves in the peripheral region of a cell mass should be less cohesive than those
170 positioned in the inner region. We tested the ability of RF cells to associate with aggregates
171 using a cohesion assay [39]. Briefly, a suspension of mechanically dissociated cells was shaken
172 to facilitate cell agglutination for 1.5, 3, and 5 h, and the number of single unattached cells was
173 quantified (Figure 1*E* left, see SI Methods). We found that cells in the bacterial suspension or
174 growth medium were less cohesive (Figure 1*E* left) than those in the phosphate buffer (Figure 1*E*
175 left, Table S1: GLM and analysis of deviance, Buffer 5 h versus Bacteria 5 h: adjusted $P < 0.0001$,
176 Buffer 5 h versus Growth medium 5h: adjusted $P < 0.0001$) as expected [40]. In addition, we
177 found that the ratio of prespore cells in the unattached cells within the phosphate buffer (55%)
178 was lower than that in the non-adhesive control (82%) (Figure 1*E* right), indicating that non-
179 refed prespore cells are cohesive than prestalk cells in line with earlier literature [41]. On the
180 other hand, refed prespore cells were less cohesive comparable to that of the non-adhesive
181 control (Figure 1*E* right, Table S1: GLM and analysis of deviance, Buffer+EDTA versus Bacteria 5
182 h: adjusted $P = 0.572$). The lower cohesiveness of prestalk cells relative to prespore cells (Figure
183 1*E* right) and comparably reduced cell-cell cohesivity in refed cells (Figure 1*E* left) are consistent
184 with the peripheral positioning (Figure 1*B*,*C*).
185 Positional bias was also evident during the culmination (4–6 h after plating) in the
186 stalk region. In addition to the main stalk, stalk cells of *D. discoideum* constitute three distinct
187 cell types: The upper and lower cups and basal disc (Figure 2*A*) [24]. The cell mass elongated
188 into a finger-like form with a prespore cell mass between the upper and lower cups (Figure 2*B,C*,
189 Figure S3*B*, Movie S3), and the normal pattern was observed in NF cells (Figure 2*B*: NF+NF). In
190 contrast, in RF+NF populations, both prespore and prestalk cells of RF cells were abundant in the
191 lower cup region (Figure 2*B*, Figure S3*B*, Movie S4: RF3+NF, RF5+NF). Accordingly, the positional
192 frequency of prespore and prestalk cells was anti-correlated in NF+NF, and positively correlated
193 in RF+NF (Figure 2*B,* Table S1: GLM with gamma error, NF+NF: slope = -2.03 ± 0.26, RF5+NF:
194 slope = 3.70 ± 0.31). Later, RF cells formed the lower cup and basal disc but were excluded from
195 the upper cup and main stalk (Figure 2*C*, RF3+NF). In contrast to our standard condition (RF cells
196 were the minority; Figure 2*C*, RF3+NF), when RF cells were the majority, refed prespore and
197 prestalk cells were positioned according to their original cell fate (Figure 2*C*, RF3(Fl+):NF(Fl-) =
198 70:30).
199 In the terminal differentiation (8 to 10 h after plating), the ectopic positioning of RF
200 cells was most notable in the basal disc region, which consists mainly of secreted cellulose and
201 vacuolating non-viable cells [42, 43]. In the controls ('No-dissociation', NF+NF), the basal disc
202 was occupied by cells of prestalk-origin (Figure 2*D,E*) as expected [44]. On the other hand, in
203 RF+NF (Figure 2*D,E*), RF cells of both prestalk and prespore origins were found at the basal disc
204 (Figure 2*D,E*, Table S1, NF+NF versus RF5+NF: *t*-test, adjusted $P < 0.0001$). In addition, cells
205 scattered around the base [45] were amoeboid and showed random movement (Movie S5),
206 indicating escape from death as stalks. In the controls, these scattered cells were of prestalk
207 origin (Figure 2*F*,*G*: 'No-dissociation', NF+NF), whereas in RF+NF (Figure 2*F,G*: RF3+NF, RF5+NF),
208 RF cells of both prespore and prestalk origins were found (Figure 2*F,G,* Table S1: NF+NF versus
209 RF5+NF: *t*-test, adjusted $P < 0.0001$). At the terminal differentiation, a higher proportion of RF
210 cells were allocated to the solitary amoeboid cells rather than spores, compared to NF cells in
211 the mixed cell population of RF+NF (Figure S4). These results (Figure 2*F,G,* Figure S4, Movie S5)

212 indicate that the final survivors at the terminal phase were solitary cells (amoeba) and social
213 cells (spores).
214
215 **The growth cost of the social commitment**
216 Our refeeding experiments indicate that *Dictyostelium* cells that dedifferentiate precociously are
217 penalized by being assigned the role of the non-viable stalk (Figure 1,2). Here, we went on to
218 investigate a basic question of how the social commitment imposes individual cells growth
219 costs. Cells were released from the commitment by mechanical dissociation and two types of
220 growth costs were estimated: Growth delay incurred by fruiting body formation (d) and lag time
221 for spore germination (λ) (Figure 3*A*). We found no significant growth differences due to the
222 growth delay d ('Refed & No-dissociation' versus 'Refed & Dissociation': GLM and analysis of
223 deviance, $P = 0.069$); however, as the lag time for spore germination (λ), the socially committed
224 cells consumed approximately 9 h longer time to start cell growth than the de-committed cells
225 (Figure 3*B*, Table S1: Estimated lag time between cell inoculation and initiation of cell growth,
226 'Refed & Dissociation': 15.24 ± 4.27 h, 'Refed & No-dissociation': 23.97 ± 4.35 h). The significant
227 growth delay highlights the cost for individual cells of remaining in the social group under
228 nutrient-rich environments (Figure 3*B*, Table S1: 'Refed & No-dissociation' versus 'Refed &
229 Dissociation': GLM and analysis of deviance, $P < 0.003$).
230
231 **Model analysis for evolutionary maintenance of the social commitment**
232 If the de-committed strain is rewarded by such a growth advantage (Figure 3), how stable is
233 social commitment against adverse evolutionary pressures? We analyze whether a rare mutant
234 cell that reverts to a solitary state could invade a wild-type population with the framework of
235 adaptive dynamics [46, 47]. We considered a sufficiently large population of haploid and
236 asexually reproducing cells that are exposed to nutrient recovery at each slug stage. The
237 evolutionary trait is a degree of association with other cells, x ($0 \leq x \leq 1$) (Table S3). Cells with
238 any of the traits normally commit to the differentiation, and then express the trait x at the slug
239 stage. Both cell fate and fitness are decided according to x. A wild-type cell has the trait $x =$
240 x_{wt}, where its default value is $x_{wt} = 1$ indicating full social commitment. According to the value
241 of x, a single cell simultaneously has probabilities to be a spore, stalk, and solitary cell. The
242 probabilities are equivalent to cell fate ratios in a clonal population with the trait x. The cell fate
243 ratios of the full social commitment ($x = 1$) are designated as spore: $SP_{initial} = 0.6$, stalk:
244 $ST_{initial} = 0.2$, and solitary: $Sol_{initial} = 0.2$, respectively (for suitability of the parameters see,
245 Figure S5).
246 We consider that invasion of a rare mutant cell with the trait $x' = x_{wt} + \varepsilon$, ($\varepsilon$ is a
247 sufficiently small negative value). The rare mutant cell makes a chimera slug with the wild-type
248 cells, and expresses the trait x' within the slug and reverts to a solitary state. We assume that x
249 controls most of cohesion proteins as a 'master regulator', i.e., $x = 1$ indicates fully cohesive,
250 and $x = 0$ is complete degradation of cohesion proteins (Figure 4*A*). According to previous
251 study and our experimental results (Figure 1*E*) [41], cohesion of each cell fate is assumed to be
252 distinctively different, and the highest is prespore, followed by in the order of prestalk, solitary
253 cell (hereafter the allocation is referred to as 'canonical allocation'). When a cell has a reduced
254 trait value ($x < 1$), the trait expression may induce cohesion degradation as the conceptual

illustration of distribution shifts in Figure 4*A*. For example, the prespore cell after the trait expression will exhibit reduced cohesion similar to an original prestalk or solitary cell. From our refed experiments (Figure 1,2), a cell is assumed to play a cell fate role as determined by its own reduced cohesivity, rather than its original fate. Thus, given the order of cohesion (Figure 1*E*) [41], a cell changes a role via evolution x in the order of prespore, prestalk, and solitary cell (Figure 4*B*). With these evolutionary steps being described by the following differential equations:

$$\frac{dP(SP|x)}{dx} = k_1 P(SP|x),$$
$$\frac{dP(ST|x)}{dx} = -k_1 P(SP|x) + k_2 P(ST|x), \quad (1)$$
$$\frac{dP(Sol|x)}{dx} = -k_2 P(ST|x),$$

where $P(Z|x)$ is the probability of a cell with the trait x taking fate *Z* (SP: Spore, ST: Stalk, Sol: Solitary cell). Note that $P(SP|x) + P(ST|x) + P(Sol|x) = 1$. k_1, and k_2 are the rates of cell fate transition ($k_1 > 0$, $k_2 > 0$). If $k_1 \gg k_2$, decrement of the spore probability is quick but that of stalk probability is slow in the evolution (Eq. **1,** Figure 4*B*). On the other hand, if $k_1 \ll k_2$, vice versa. Our refed experiments (Figure 2) support the assumption $k_1 \gg k_2$, because we observed a much smaller number of RF cells in the prespore region of early fruiting bodies (quick $P(SP|x)$ decrement) but abundant RF cells in the stalk region (lower cup and basal disc) (slow $P(ST|x)$ decrement). We select default values as $k_1 = 14.6$ and $k_2 = 6.3$ (see, SI text).

Invasion fitness of the mutant cell is

$$W(x'; x_{wt}) = f(x'; x_{wt}) - f(x_{wt}; x_{wt}), \quad (2)$$

where, $f(x'; x_{wt})$ is the survival probability of the mutant, and $f(x_{wt}; x_{wt})$ is that of the wild-type cell (Table S3). Both $f(x'; x_{wt})$ and $f(x_{wt}; x_{wt})$ are defined as the sum of the probabilities of becoming a spore (social fitness) and a solitary amoeboid cell (solitary fitness) as follows,

$$f(x) = P(SP|x) + g\, P(Sol|x), \quad (3)$$

where, g represents the additional weight of solitary fitness as defined by amounts of nutrients. Thus, for simplicity, amounts of nutrients directly contribute the solitary fitness. The equation Eq. **3** simply describes the allocation between solitary and social life, and we also consider another formulation that assumes explicit altruism (Figure S6) shown fundamentally the same result as that from Eq. **3**.

The invasion fitness when the mutant interacts with the wild-type cell with $x_{wt} = 1$ (Figure 4*C*) showed a fitness valley under the intermediate nutrient-rich condition (e.g., $g = 1$), owing to the transient increase in the stalk fate probability during the evolution. In the starved condition ($g = 0$), the mutant is always disadvantageous, while in the nutrient-rich condition ($g = 10$) the mutant rapidly evolves (Figure 4*C*). Ecology-evolution-environment diagram [47] in Figure 4*D* shows that the evolutionary equilibrium is $x = 0$ or $x = 1$ depending on the starting point of the evolution. The point where the selection gradient vanishes, i.e., 'evolutionarily singular' [46, 47] x^* is in the 'bottom' of the valley (evolutionary repellor) (Figure 4*D,* 'Canonical allocation'), and neither an evolutionarily stable strategy (ESS) [48] nor convergence stable [46, 49] under our assumed condition ($k_1 \gg k_2$) (for detail, see SI text and Figure S7). Thus, the model predicts that once the wild-type cells acquire complete social

commitment ($x = 1$), mutant invasion is blocked under a wide range of intermediate nutrient-rich conditions.

The fitness valley (Figure 4*C,D*) was caused by a direct consequence of division of labor that assigns each cell fate with a degree of cell-cell cohesion in the order of prespore $>$ prestalk $>$ solitary cell (canonical allocation). If the social amoeba were to have an alternative type of allocation rule: With cohesion order of prestalk $>$ prespore $>$ solitary cell (reverse allocation), and with prespore $=$ prestalk $>$ solitary cell (random allocation), these systems did not prevent invasion of the solitary reversion mutant (Figure 4*D*). In the reverse allocation system, an evolutionary singular point x^* is the partially solitary state (Figure 4*D*, 'Reverse allocation') and is ESS and convergence stable under our assumed condition ($k_1 \gg k_2$) (see SI text), indicating that cells make more spores by the solitary reversion in exchange for small amounts of robustness of a fruiting body. In the random allocation system, there is no singular point (Figure 4*D*, 'Random allocation'). Taken together, only the canonical allocation system can protect the social commitment under nutrient-rich conditions.

Finally, to understand the range of the social defense, invasion of a cheating mutant is investigated in addition to the solitary reversion mutant. We consider a rare cheating mutant cell that has a higher probability to be a spore than the wild-type cell within a chimera. An evolutionary trait i is additional spore investment at the slug stage. The wild-type trait is $i = i_{wt}$ where $i_{wt} = 0$ is the default value, and the cheating mutant trait is $i = i' = i_{wt} + \theta$, (θ is a sufficiently small positive value). We especially focused on the detailed developmental process of the social amoeba: a slug migrates toward the light, probably to reach the soil surface, where spore dispersal is more likely [24]. The migrating slug induces a series of cell fate transitions closely resembling those associated with the canonical allocation: There is a sub-population of prestalk cells left behind from a slug [50], which are compensated by trans-differentiation of prespore to prestalk cells [51]. Cell fate transition over the migration time t is described as differential equations (Eq. **S17**-**S19** in SI text). The invasion fitness of the cheating mutant $W(i'; i_{wt})$ is the sum of spore and solitary probabilities (Eq. **S21**, Eq. **S22** in SI text). The selection gradient (Eq. **S23** in SI text) was constant with respect to i, and we found the condition that the cheating mutant evolves (red lines in Figure 5, Eq. **S24**-**S26** in SI text). The model shows that evolution of the cheating mutant is suppressed under nutrient-rich conditions in the canonical allocation, while in the reverse allocation the evolution is suppressed under starved conditions but enforced under nutrient-rich conditions. In the random allocation, cheating always evolves (Figure 5). Thus, if the social amoeba experiences only starved conditions, the reverse allocation is suitable; however, under nutrient-rich conditions, the canonical allocation will demonstrate the comprehensive defense capacity.

Discussion

Maintenance of cooperation is inextricably linked to the choice of social members to be dispersed from a society [52]. We show the choice of the leavers can canalize 'point of no return' in the social evolution [12, 13]. Our results suggest that *Dictyostelium* employs the division of labor in which cells with a less cohesive propensity become altruists. The dedifferentiating *Dictyostelium* cells take a prestalk-like cell state through interaction with

differentiating cells (Figure 1,2); thus, the system penalizes precocious solitary reversion (Figure 4). Unlike policing, which entails inescapable costs in general [2], the penalization occurs naturally through fruiting body formation and the social amoeba seems not to pay explicit costs.

What evolutionary trajectory did organisms follow to cross 'point of no return' is one of fundamental questions. In addition to the solitary reversion mutant, our model (Figure 5) showed that the division of labor of *Dictyostelium* can effectively reduce the advantage of cheating mutants, which is consistent with earlier experimental observations [53]. From these results, it is tempting to speculate that the social amoeba could have first acquired the canonical allocation to suppress cheating, and this in turn penalized solitary reversion as a byproduct. Given that the dedifferentiation process is regulated by several thousand genes [28, 54], the presence of the fitness valley (Figure 4*C,D*) acts as a strong resistance to the social commitment breaking down. Furthermore, for microbes with large clonal populations, the chance of crossing the fitness valley through genetic drift is slim [55] without additional mechanisms [56]. On the other hand, the fitness valley may work only at the early stage of invasion due to its frequency dependency; The de-committed cells were penalized when they are in the minority (~15% of the population) but not in the majority (70%~) (Figure 2*C*). Even if the social amoeba crossed the valley, the evolutionary progression may be too slow to manifest itself, since the dedifferentiation process is known to be robust to genetic perturbation [54]. Future experimental evolution studies should clarify the evolutionary process given their genetic background and developmental processes.

How the social commitment of *Dictyostelium* is maintained has been a long-standing question ever since the observation was first reported [27]. Our experimental results suggest an interesting cellular dynamics-based mechanism as to how this is implemented. The initial prestalk-like positioning of refed cells to the mound periphery (Figure 1*B*) can be explained based on the mechanism of cell segregation [38] by differential adhesion of non-refed cells and refed cells (Figure 1*E*). Later, the refed cells were positioned at the base of the mound (Figure S3*A*), which then formed the lower cup (Figure 2*B*) and the basal disc (Figure 2*D*). The basal disc and lower cup are well-known terminal states of prestalk cells [44, 57], however, how cells are positioned at these locations is not well understood. The localization of refed cells is distinct from that of the primary stalk cells but similar to that of the 'anterior-like cells' [57–60] – a small percentage of poorly characterized prestalk subtype that constitutes the basal disc, the lower cup, and the upper cup. The lack of refed cells from the upper cup makes it distinct from the anterior-like cells. This, as well as its absence from the main stalk, may be related to reduced sensitivity to cAMP due to the decreased *carA* gene expression in the refed cells (Figure 1*D*), as low sensitivity to cAMP facilitates re-differentiation of prespore cells to lower cup cells and inhibits prestalk cells positioning to the upper cup [61].

Cooperation is a fundamental force that leads to the emergence of collective-level selection units [62, 63]. Paradoxically, the fact that individuals are allowed to choose a solitary strategy among other options, such as to cooperate or to cheat, can in turn maintain cooperation by reducing cheating interest [64]. In cellular cooperation, the presence of cells ungrouped can compensate for the cost of aggregation [65], and facilitate coexistence of diverse fruitification traits as a bet-hedging strategy to variable environmental conditions [66, 67]. However, such a solitary cell type may not be sufficient to maintain cooperation in

382 environments that act favorably for solitary growth (Figure 3*B*), for example, relatively long
383 nutrient-rich conditions interrupted by brief intervals of starvation. Under such conditions,
384 precocious reversion to a solitary state would be beneficial for individual cells. This notion is
385 supported not only by our growth assay (Figure 3*B*) but also by the fact that there exist cells that
386 are left behind from a slug that can grow quickly after nutrient recovery [68]. The social system
387 appears to include a certain proportion of a solitary cell type in the first place as a bet-hedging
388 strategy, but for those that are socially committed, there is little payoff from quitting
389 cooperation because of their specific division of labor (Figure 4). Our study provides a simple
390 explanation for the emergence of collective behavior that is apparently counterintuitive in terms
391 of individual-level fitness.
392
393
394 **Materials and Methods**
395 **Refeeding experiments**
396 Strains expressing cell fate markers were constructed from AX4 cells. To obtain slug-stage cells,
397 vegetative cells were washed with the phosphate buffer (PB) and applied to a 1% PB agar plate
398 and incubated for 18 h. PB containing 20 mM EDTA was applied to the slugs, and the cells were
399 mechanically dissociated by repeated pipetting and passed through a 23 G needle and 40 μm
400 cell strainer. For refeeding, dissociated cells were co-suspended at 2 to 3 $\times$ 10^6 cells/mL with
401 the concentrated *E. coli* B/r. NF cells were cells suspended in PB immediately after dissociation.
402 The mixed cell suspension contains RF and NF cells at 1 to 2 $\times$ 10^6 cells/mL was plated on a
403 glass-bottomed dish (MatTek, Ashland, MA, USA) covered with a thin sheet of 1% PB agar.
404 Confocal fluorescence images were taken using an inverted confocal microscope (Nikon A1+)
405 and Z-slices were obtained using a Ti Z-drive. See also SI Methods.
406 **Real-time PCR analysis**
407 Dissociated slug cells were suspended in each solution, and shaken at 120 rpm, and harvested at
408 the selected time points. Quantitative PCR amplification (qPCR) was performed using a qPCR
409 thermocycler (ABI7500, Applied Biosystems) with primer pairs and fluorescent beacons
410 (TaqMan probe MGB, Applied Biosystems) (Table S2). The levels of relative gene expression
411 were calculated from the amplification value at the threshold cycle and the relative standard
412 curve for each gene, followed by normalization by *rnlA* amplification as an endogenous control.
413 **Growth assay**
414 Vegetative cells were starved at 2 $\times$ 10^6 cells/cm^2. *E. coli* suspension was applied either
415 directly to the slugs or after mechanical dissociation. After 30h incubation, the samples were
416 harvested and washed 2 times to remove the bacteria. Then, 3 $\times$ 10^6 cells were transferred
417 into 10 mL of the growth medium and shaken at 120 rpm. The cell number at different times
418 was measured using a hemocytometer.
419 **Statistical analysis**
420 *P*-values from multiple comparisons were adjusted using Holm's method. A generalized linear
421 model (GLM) and analysis of deviance for the fit were performed for the analysis listed in Table
422 S1.
423
424

Acknowledgments

We thank K. Kaneko for providing critical comments, T. Fujimori, T. Yoshida, and lab members for discussion and technical advice, and A. Nakajima for the microscopy setup. This work was supported by the Platform for Dynamic Approaches to Living System from the Ministry of Education, Culture, Sports, Science, and Technology, Japan to Y.S., M.S., and S.S.; and by a Grant-in-Aid for Challenging Exploratory Research (Nos. 16K14805) from the Japan Society for the Promotion of Science (JSPS) to Y.S., and M.S. and JSPS Grant-in-Aid 18H04759 and Japan Science and Technology Agency (JST) CREST JPMJCR1923 to S.S..

476 **References**
477

478 [1] Hamilton WD. The genetical evolution of social behaviour. Journal of Theoretical Biology.
479 1964;7(1):1–52. doi:10.1016/0022-5193(64)90038-4

480 [2] Frank SA. Mutual policing and repression of competition in the evolution of cooperative
481 groups. Nature. 1995;377(6549):520–522. doi:10.1038/377520a0

482 [3] West SA, Griffin AS, Gardner A, Diggle SP. Social evolution theory for microorganisms. Nature
483 Reviews Microbiology. 2006;4(8):597–607. doi:10.1038/nrmicro1461

484 [4] Hallatschek O, Hersen P, Ramanathan S, Nelson DR. Genetic drift at expanding frontiers
485 promotes gene segregation. Proceedings of the National Academy of Sciences of the United
486 States of America. 2007;104(50):19926–19930. doi:10.1073/pnas.0710150104

487 [5] Buttery NJ, Jack CN, Adu-Oppong B, Snyder KT, Thompson CRL, Queller DC, Strassmann JE.
488 Structured growth and genetic drift raise relatedness in the social amoeba *Dictyostelium*
489 *discoideum*. Biology letters. 2012;8(5):794–797. doi:10.1098/rsbl.2012.0421

490 [6] Smukalla S, Caldara M, Pochet N, Beauvais A, Guadagnini S, Yan C, Vinces MD, Jansen A,
491 Prevost MC, Latgé J-P, et al. *FLO1* is a variable green beard gene that drives biofilm-like
492 cooperation in budding yeast. Cell. 2008;135(4):726–737. doi:10.1016/j.cell.2008.09.037

493 [7] Ho HI, Hirose S, Kuspa A, Shaulsky G. Kin recognition protects cooperators against cheaters.
494 Current biology. 2013;23(16):1590–1595. doi:10.1016/j.cub.2013.06.049

495 [8] Velicer GJ, Kroos L, Lenski RE. Loss of social behaviors by *Myxococcus xanthus* during
496 evolution in an unstructured habitat. Proceedings of the National Academy of Sciences of the
497 United States of America. 1998;95(21):12376–12380.

498 [9] Danforth BN. Evolution of sociality in a primitively eusocial lineage of bees. Proceedings of
499 the National Academy of Sciences. 2002;99(1):286–290. doi:10.1073/pnas.012387999

500 [10] James TY, Kauff F, Schoch CL, Matheny PB, Hofstetter V, Cox CJ, Celio G, Gueidan C, Fraker
501 E, Miadlikowska J, et al. Reconstructing the early evolution of Fungi using a six-gene phylogeny.
502 Nature. 2006;443(7113):818–822. doi:10.1038/nature05110

503 [11] Schirrmeister BE, Antonelli A, Bagheri HC. The origin of multicellularity in cyanobacteria.
504 BMC Evolutionary Biology. 2011;11(1):45. doi:10.1186/1471-2148-11-45

505 [12] Wilson EO. The Insect Societies. Cambridge: Belknap Press; 1971. (Belknap Press).

506 [13] Wilson EO, Hölldobler B. Eusociality: Origin and consequences. Proceedings of the National
507 Academy of Sciences of the United States of America. 2005;102(38):13367–13371.
508 doi:10.1073/pnas.0505858102

509 [14] Libby E, Ratcliff WC. Ratcheting the evolution of multicellularity. Science.
510 2014;346(6208):426–427. doi:10.1126/science.1262053

511 [15] Libby E, Conlin PL, Kerr B, Ratcliff WC. Stabilizing multicellularity through ratcheting.
512 Philosophical Transactions of the Royal Society B: Biological Sciences.
513 2016;371(1701):20150444. doi:10.1098/rstb.2015.0444

514 [16] Ratcliff WC, Denison RF, Borrello M, Travisano M. Experimental evolution of multicellularity.
515 Proceedings of the National Academy of Sciences. 2012;109(5):1595–1600.
516 doi:10.1073/pnas.1115323109

517 [17] Bull JJ, Charnov EL. On irreversible evolution. Evolution. 1985;39(5):1149–1155.
518 doi:10.1111/j.1558-5646.1985.tb00455.x

519 [18] Santorelli LA, Thompson CRL, Villegas E, Svetz J, Dinh C, Parikh A, Sucgang R, Kuspa A,
520 Strassmann JE, Queller DC, et al. Facultative cheater mutants reveal the genetic complexity of
521 cooperation in social amoebae. Nature. 2008;451(7182):1107–1110. doi:10.1038/nature06558

522 [19] Khare A, Santorelli LA, Strassmann JE, Queller DC, Kuspa A, Shaulsky G. Cheater-resistance is
523 not futile. Nature. 2009;461(7266):980–982. doi:10.1038/nature08472

524 [20] Manhes P, Velicer GJ. Experimental evolution of selfish policing in social bacteria.
525 Proceedings of the National Academy of Sciences of the United States of America.
526 2011;108(20):8357–8362. doi:10.1073/pnas.1014695108

527 [21] Riley MA, Wertz JE. Bacteriocins: Evolution, Ecology, and Application. Annual Review of
528 Microbiology. 2002;56(1):117–137. doi:10.1146/annurev.micro.56.012302.161024

529 [22] Danilova N. The evolution of immune mechanisms. Journal of Experimental Zoology Part B:
530 Molecular and Developmental Evolution. 2006;306B(6):496–520. doi:10.1002/jez.b.21102

531 [23] Bonner JT. The Cellular Slime Molds. Princeton: Princeton University Press; 1967.
532 doi:10.1515/9781400876884

533 [24] Kessin RH. Dictyostelium. Cambridge: Cambridge University Press; 2001. (Cambridge
534 University Press). doi:10.1017/cbo9780511525315

535 [25] Strassmann JE, Zhu Y, Queller DC. Altruism and social cheating in the social amoeba
536 *Dictyostelium discoideum*. Nature. 2000;408(6815):965–967. doi:10.1038/35050087

537 [26] Katoh M, Chen G, Roberge E, Shaulsky G, Kuspa A. Developmental Commitment in
538 *Dictyostelium discoideum*. Eukaryotic Cell. 2007;6(11):2038–2045. doi:10.1128/ec.00223-07

539 [27] Raper KB. Pseudoplasmodium formation and organization in *Dictyostelium discoideum*. J
540 Elisha Mitchell Sci Soc. 1940;56:241–282.

541 [28] Katoh M, Shaw C, Xu Q, Driessche NV, Morio T, Kuwayama H, Obara S, Urushihara H,
542 Tanaka Y, Shaulsky G. An orderly retreat: Dedifferentiation is a regulated process. Proceedings
543 of the National Academy of Sciences of the United States of America. 2004;101(18):7005–7010.
544 doi:10.1073/pnas.0306983101

545 [29] Gilbert OM, Queller DC, Strassmann JE. Discovery of a large clonal patch of a social amoeba:
546 implications for social evolution. Molecular Ecology. 2009;18(6):1273–1281. doi:10.1111/j.1365-
547 294x.2009.04108.x

548 [30] Chen G, Zhuchenko O, Kuspa A. Immune-like Phagocyte Activity in the Social Amoeba.
549 Science. 2007;317(5838):678–681. doi:10.1126/science.1143991

550 [31] Newell PC, Longlands M, Sussman M. Control of enzyme synthesis by cellular interaction
551 during development of the cellular slime mold *Dictyostelium discoideum*. Journal of Molecular
552 Biology. 1971;58(2):541–554.

553 [32] Deichsel H, Friedel S, Detterbeck A, Coyne C, Hamker U, MacWilliams HK. Green fluorescent
554 proteins with short half-lives as reporters in *Dictyostelium discoideum*. Development Genes and
555 Evolution. 1999;209(1):63–68.

556 [33] Siu CH, Roches BD, Lam TY. Involvement of a cell-surface glycoprotein in the cell-sorting
557 process of *Dictyostelium discoideum*. Proceedings of the National Academy of Sciences of the
558 United States of America. 1983;80:6596–6600.

559 [34] Siu CH, Harris TJC, Wang J, Wong E. Regulation of cell–cell adhesion during *Dictyostelium*
560 development. Seminars in Cell & Developmental Biology. 2004;15(6):633–641.
561 doi:10.1016/j.semcdb.2004.09.004

562 [35] Crowley TE, Nellen W, Gomer RH, Firtel RA. Phenocopy of discoidin I-minus mutants by
563 antisense transformation in *Dictyostelium*. Cell. 1985;43(3):633–641. doi:10.1016/0092-
564 8674(85)90235-1

565 [36] Bastounis E, Álvarez-González B, Álamo JC del, Lasheras JC, Firtel RA. Cooperative cell
566 motility during tandem locomotion of amoeboid cells. Molecular Biology of the Cell.
567 2016;27(8):1262–1271. doi:10.1091/mbc.e15-12-0836

568 [37] Fujimori T, Nakajima A, Shimada N, Sawai S. Tissue self-organization based on collective cell
569 migration by contact activation of locomotion and chemotaxis. Proceedings of the National
570 Academy of Sciences of the United States of America. 2019;116(10):4291–4296.
571 doi:10.1073/pnas.1815063116

572 [38] Steinberg MS, Takeichi M. Experimental specification of cell sorting, tissue spreading, and
573 specific spatial patterning by quantitative differences in cadherin expression. Proceedings of the
574 National Academy of Sciences of the United States of America. 1994;91(1):206–209.
575 doi:10.1073/pnas.91.1.206

576 [39] Parkinson K, Bolourani P, Traynor D, Aldren NL, Kay RR, Weeks G, Thompson CRL.
577 Regulation of Rap1 activity is required for differential adhesion, cell-type patterning and
578 morphogenesis in *Dictyostelium*. Journal of Cell Science. 2009;122(3):335–344.
579 doi:10.1242/jcs.036822

580 [40] Finney RE, Mitchell LH, Soll DR, Murray BA, Loomis WF. Loss and resynthesis of a
581 developmentally regulated membrane protein (gp80) during dedifferentiation and
582 redifferentiation in *Dictyostelium*. Developmental Biology. 1983;98(2):502–509.
583 doi:10.1016/0012-1606(83)90379-2

584 [41] Lam TY, Pickering G, Geltosky J, Siu CH. Differential cell cohesiveness expressed by prespore
585 and prestalk cells of *Dictyostelium discoideum*. Differentiation. 1981;20(1–3):22–28.
586 doi:10.1111/j.1432-0436.1981.tb01151.x

587 [42] Whittingham WF, Raper KB. Non-viability of stalk cells in *Dictyostelium*. Proceedings of the
588 National Academy of Sciences. 1960;46(5):642–649. doi:10.1073/pnas.46.5.642

589 [43] Harrington BJ, Raper KB. Use of a fluorescent brightener to demonstrate cellulose in the
590 cellular slime molds. Applied Microbiology. 1968;16(1):106–113.

591 [44] Jermyn K, Traynor D, Williams J. The initiation of basal disc formation in *Dictyostelium*
592 *discoideum* is an early event in culmination. Development. 1996;122:753–760.

593 [45] Watts DJ, Treffry TE. Culmination in the slime mould *Dictyostelium discoideum* studied with
594 a scanning electron microscope. Journal of embryology and experimental morphology.
595 1976;35(2):323–333.

596 [46] Geritz SAH, Kisdi É, Meszéna G, Metz JAJ. Evolutionarily singular strategies and the adaptive
597 growth and branching of the evolutionary tree. Evolutionary Ecology. 1998;12(1):35–57.
598 doi:10.1023/a:1006554906681

599 [47] Dieckmann U, Ferrière R. Adaptive Dynamics and Evolving Biodiversity. In: Ferrière R,
600 Dieckmann U, Couvet D, editors. Evolutionary conservation biology. Cambridge, UK: Cambridge
601 University Press; 2004. p. 188–224.

602 [48] Smith JM. Evolution and the theory of games. Cambridge University Press; 1982.
603 (Cambridge University Press).

604 [49] Eshel I. Evolutionary and continuous stability. Journal of Theoretical Biology.
605 1983;103(1):99–111. doi:10.1016/0022-5193(83)90201-1

606 [50] Sternfeld J. A study of PstB cells during *Dictyostelium* migration and culmination reveals a
607 unidirectional cell type conversion process. Roux's archives of developmental biology.
608 1992;201(6):354–363. doi:10.1007/bf00365123

609 [51] Abe T, Early A, Siegert F, Weijer C, Williams J. Patterns of cell movement within the
610 *Dictyostelium* slug revealed by cell type-specific, surface labeling of living cells. Cell.
611 1994;77(5):687–699.

612 [52] Hochberg ME, Rankin DJ, Taborsky M. The coevolution of cooperation and dispersal in
613 social groups and its implications for the emergence of multicellularity. BMC Evolutionary
614 Biology. 2008;8(1):238. doi:10.1186/1471-2148-8-238

615 [53] Jack CN, Buttery N, Adu-Oppong B, Powers M, Thompson CRL, Queller DC, Strassmann JE.
616 Migration in the social stage of *Dictyostelium discoideum* amoebae impacts competition. PeerJ.
617 2015;3:e1352. doi:10.7717/peerj.1352

618 [54] Nichols JM, Antolovic V, Reich JD, Brameyer S, Paschke P, Chubb JR. Cell and molecular
619 transitions during efficient dedifferentiation. eLife. 2020;9:e55435. doi:10.7554/elife.55435

620 [55] Lande R. Expected time for random genetic drift of a population between stable phenotypic
621 states. Proceedings of the National Academy of Sciences of the United States of America.
622 1985;82(22):7641–7645.

623 [56] Iwasa Y, Michor F, Nowak MA. Stochastic tunnels in evolutionary dynamics. Genetics.
624 2004;166(3):1571–1579.

625 [57] Sternfeld J. The anterior-like cells in *Dictyostelium* are required for the elevation of the
626 spores during culmination. Development Genes and Evolution. 1998;208(9):487–494.

627 [58] Sternfeld J, David CN. Cell Sorting daring Pattern Formation in *Dictyostelium*.
628 Differentiation. 1981;20(1–3):10–21. doi:10.1111/j.1432-0436.1981.tb01150.x

629 [59] Dormann D, Siegert F, Weijer CJ. Analysis of cell movement during the culmination phase of
630 *Dictyostelium* development. Development. 1996;122(3):761–769.

631 [60] Saito T, Kato A, Kay RR. DIF-1 induces the basal disc of the *Dictyostelium* fruiting body.
632 Developmental Biology. 2008;317(2):444–453. doi:10.1016/j.ydbio.2008.02.036

633 [61] Bichler G, Weijer CJ. A *Dictyostelium* anterior-like cell mutant reveals sequential steps in the
634 prespore prestalk differentiation pathway. Development. 1994;120(10):2857–2868.

635 [62] Smith JM, Szathmáry E. The Major Transitions in Evolution. New York: Oxford University
636 Press; 1995. (Oxford University Press).

637 [63] Michod RE, Roze D. Cooperation and conflict in the evolution of individuality. III. Transitions
638 in the unit of fitness. In: Nehaniv CL, editor. Mathematical and Computational Biology:
639 Computational Morphogenesis, Hierarchical Complexity, and Digital Evolution. American
640 Mathematical Society; 1999. p. 47–92.

641 [64] Hauert C, Monte SD, Hofbauer J, Sigmund K. Replicator dynamics for optional public good
642 games. Journal of Theoretical Biology. 2002;218:187–194. doi:10.1006/yjtbi.3067

643 [65] Garcia T, Doulcier G, Monte SD. The evolution of adhesiveness as a social adaptation. eLife.
644 2015;4:e08595. doi:10.7554/elife.08595.001

645 [66] Dubravcic D, Baalen M van, Nizak C. An evolutionarily significant unicellular strategy in
646 response to starvation in *Dictyostelium* social amoebae. F1000Research. 2014;3:133.
647 doi:10.12688/f1000research.4218.2

648 [67] Tarnita CE, Washburne A, Martinez-Garcia R, Sgro AE, Levin SA. Fitness tradeoffs between
649 spores and nonaggregating cells can explain the coexistence of diverse genotypes in cellular
650 slime molds. Proceedings of the National Academy of Sciences of the United States of America.
651 2015;112(9):2776–2781. doi:10.1073/pnas.1424242112

652 [68] Kuzdzal-Fick JJ, Foster KR, Queller DC, Strassmann JE. Exploiting new terrain: an advantage
653 to sociality in the slime mold *Dictyostelium discoideum*. Behavioral Ecology. 2007;18(2):433–
654 437. doi:10.1093/beheco/arl102

655

656

657 **Figures**

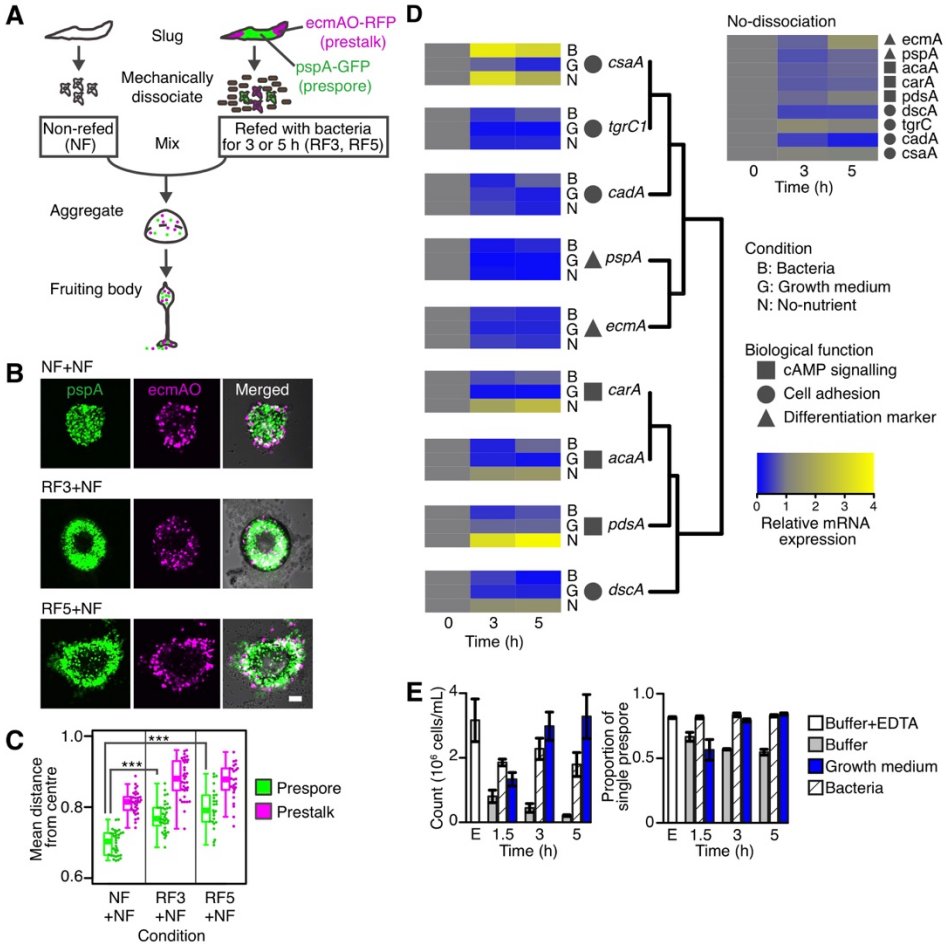

658
659 **Figure 1. Prestalk-like positioning and cell-state of refed cells.** (*A*) A schematic of refeeding
660 and reaggregation of a cell mixture. Dissociated cells were shaken with *E. coli* for 3 or 5 h
661 (Refed: RF3, RF5), washed and mixed with non-refed cells (Non-refed: NF). RF cells harbored
662 prespore (pspA-GFP, green) and prestalk (ecmAO-RFP, magenta) markers. (*B*) Representative
663 images of mixed aggregates 1.5–2 h after plating (pspA: GFP-channel, ecmAO: RFP-channel,
664 Merged: bright-field and fluorescence images). 'NF+NF': a mixture of NF cells with and without
665 the cell-type reporter as a control condition. 'RF3+NF' and 'RF5+NF': Mixture of NF cells and RF3
666 or RF5 cells, respectively at RF:NF = 15:85 ratio. A scale bar = 50 µm. (*C*) Normalized mean
667 distance between the aggregate center and cells of prestalk- or prespore-origin. The sample size
668 N (biological replicate, aggregates): NF+NF = (4, 34), RF3+NF = (4, 35), RF5+NF = (3, 25). Circles:
669 Values for individual aggregates, lines inside of box plots: The median values. *** $P < 0.0001$ by
670 *t* test. (*D-E*) Cell-state change incurred by refeeding. (*D*) qRT-PCR analysis. Gene expression
671 levels of dissociated cells in bacterial suspension 'B', growth medium 'G', non-nutrient buffer 'N'
672 (left panel). Unperturbed slugs 18 h into starvation onward ('No-dissociation': Upper right
673 panel). Gene expression levels were normalized by the 0 h point. Gene targets were clustered
674 hierarchically. The sample size N = 3 are biological replicates. (*E*) Differences in cell
675 cohesiveness between RF and NF cells. The number of single cells within a sample (left panel).

676 The proportion of single prespore cells in the total single cells within a sample (right panel). 'E':
677 Cells in the phosphate buffer containing EDTA (Buffer+EDTA) as a control (most cells were in a
678 single state). The number (1.5, 3, and 5) indicates hours shaken in suspensions. The sample size
679 N =3 are biological replicates, with 380–5966 cells per condition. Error bars are standard error.
680

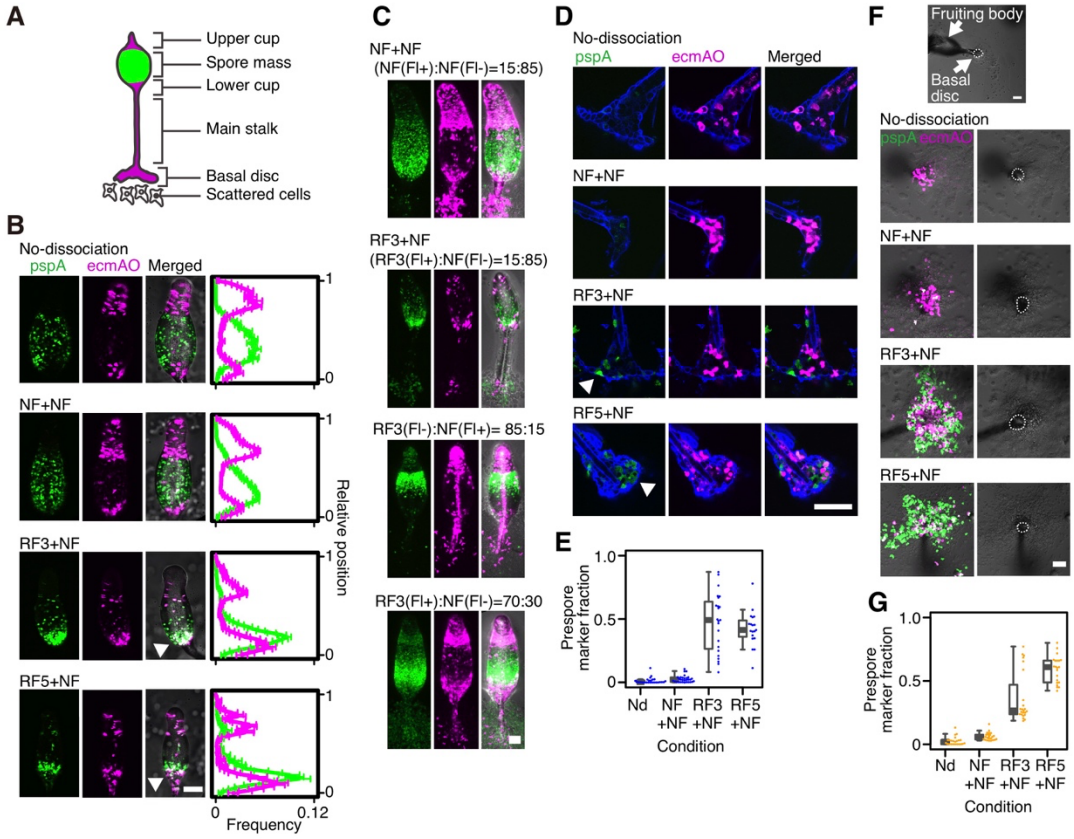

Figure 2 Refeeding redirects cells to the role of prestalk subtype. (*A*) A schematic illustration of the fruiting body. (*B*) Snapshots of the upper region of early fruiting bodies (left). Frequency of prestalk (magenta line) and prespore (green) marker-positive pixels along the anterior-posterior axis (right). No-dissociation (Nd): A fruiting body formed by unperturbed cells. In RF3+NF and RF5+NF, RF cells were found exclusively at the lower cup (arrowheads). The sample size N (biological replicate, fruiting body number): N: Nd = (2, 14), NF+NF = (3, 24), RF3+NF = (3, 20), RF5+NF = (3, 13). For abbreviations, see also Figure 1. (*C*) Early fruiting bodies consisted of different ratios of RF3 and NF cells. Fl+, Fl-: with/without cell-type markers, respectively. (*D*) Fluorescent images of the basal disc. Images of stalk cellulose staining (blue, calcofluor white) were merged with fluorescence images (pspA, ecmAO). Note RF cells of prespore origin are found in the basal disc (RF3+NF and RF5+NF) (arrowheads). (*E*) The ratio of prespore marker-positive to prestalk region in the basal disc. N: Nd = (3, 26), NF+NF = (3, 30), RF3+NF = (3, 23), RF5+NF = (3, 19). (*F*) Representative images of the basal region of fruiting bodies. Note RF cells (fluorescent cells, left panel) scattered around the basal discs (white circles, right panel) in RF3+NF and RF5+NF. (*G*) The ratio of prespore marker-positive region to prestalk region in the scattered cells. N: Nd = (3, 23), NF+NF = (3, 23), RF3+NF = (3, 23), RF5+NF = (3, 21). All scale bars = 50 µm. Error bars: Standard error.

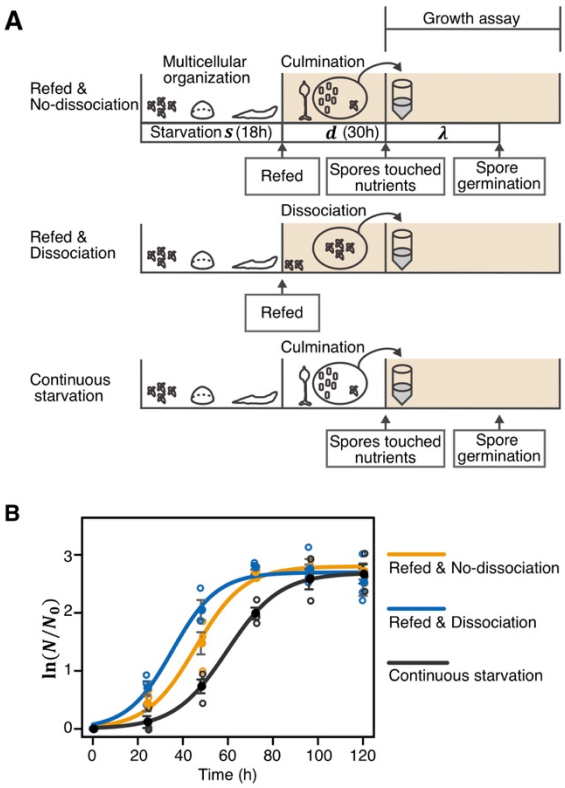

Figure 3 Social commitment imposes growth costs under nutrient recovery. (*A*) The schematic of the growth assay. Cells in the slug stage (s =18 h) are exposed to nutrient recovery. Cells were released from the commitment by mechanical dissociation. Under the social commitment ('Refed & No-dissociation' and 'Continuous starvation'), cells ignore nutrients and develop into a fruiting body. Thus, except for only rare non-aggregated cells, the socially committed cells would bear two types of growth costs: Growth delay incurred by fruiting body formation (d) and lag time for spore germination (λ). Without social commitment ('Refed & Dissociation'), cells quickly restart growing immediately after refeeding. After 30h incubation (d) for the fruiting body maturation, amoeboid cells and spores were harvested and transferred into the growth medium to estimate growth costs. (*B*) Growth assay. 'Refed & No-dissociation' (orange): A growth curve of cells from the non-dissociated refed slugs, 'Refed & Dissociation' (blue): Cells from refed slugs that were dissociated, 'Continuous starvation' (black): cells from uninterrupted slugs under continued starvation. $\ln(N/N_0)$: Logarithm of relative population size that was normalized by the initial cell number. The error bars: Relative error. Circles: Individual values from three biological replicates. Regrowth of refed cells from non-dissociated slugs was significantly delayed compared to that of dissociated slugs (GLM, $P < 0.003$).

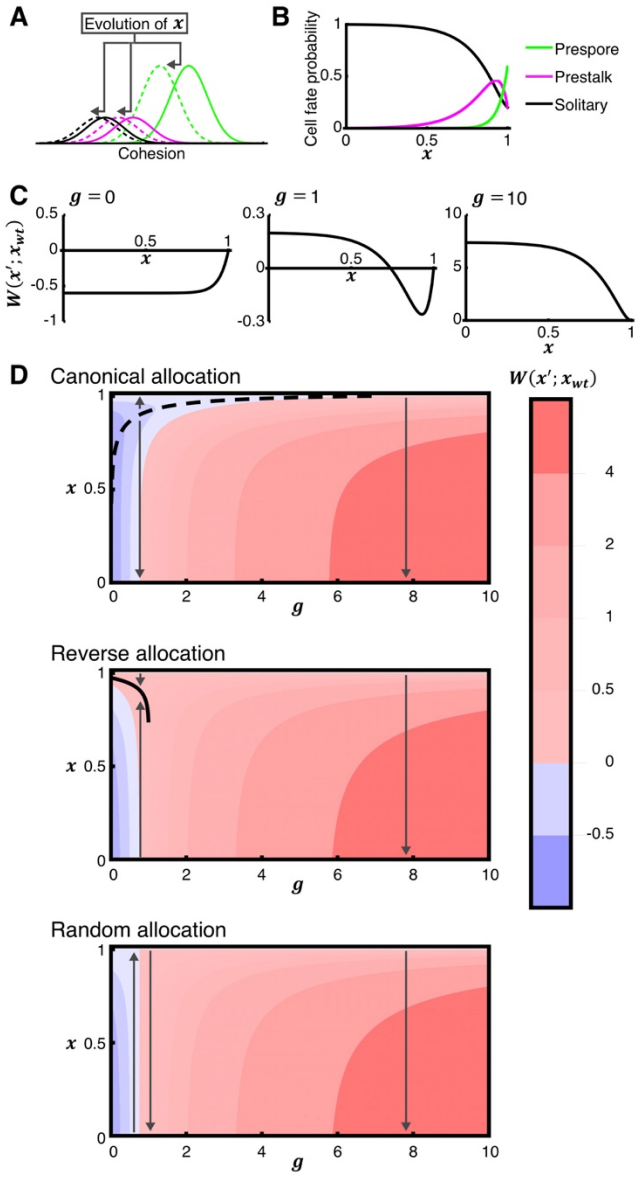

Figure 4 Social commitment in *Dictyostelium* is an evolutionarily stable strategy. (*A*) An intuitive explanation of cell fate transitions via the evolution of trait x. The trait x ($0 \leq x \leq 1$) is assumed to decide the cell-cell association level, which generally controls most of cohesion proteins as a 'master regulator' ($x = 1$: full social commission, $x = 0$: a solitary state, complete degradation of cohesion proteins). The solid lines indicate cohesion distributions of prespore (green), prestalk (magenta), and solitary cells (black) in the cell population. The evolution of reduced x can be illustrated as distribution shifts (dotted line). After evolution of x, prespore cells (dotted green line) will exhibit reduced cohesion similar to original prestalk and solitary cells (solid magenta and black lines). Cells are assumed to play a cell-fate role as determined by the reduced cohesion rather than the original cell fate, according to our experiments (Figure 1,2). (*B*) Evolution of x and its link to the cell fate role probability assuming division of labor that assigns each cell fate with a degree of cohesion (canonical allocation: prespore > prestalk >

solitary cell) (Eq. **1**). (*C*) The invasion fitness of the solitary reversion mutant within the wild-type population $W(x'; x_{wt})$, where the wild-type trait is $x_{wt} = 1$ under canonical allocation. g is the additional weight for the solitary fitness as defined by nutrient availability. Note that the fitness function has a valley in the intermediate nutrient condition ($g = 1$) suggesting that the mutant cannot evolve when the evolution starts from the vicinity of $x = 1$. (*D*) Evolutionary directions and equilibrium under various environmental conditions. Black lines indicate analytical predictions for the singular point x^* (dotted line: Evolutionary repellor, solid line: Evolutionary attractor). Allows indicate the direction of selection. The red and blue colors indicate invasion fitness of the mutant interacts with the wild-type cell with $x_{wt} = 1$.

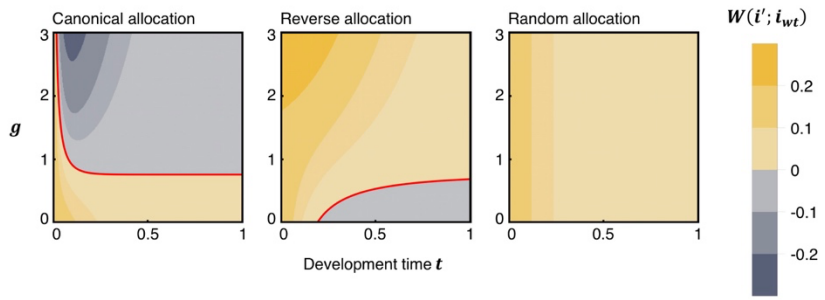

Figure 5 Division of labor in *Dictyostelium* effectively reduces cheating advantage. Evolutionary trait i describes additional spore investment, i_{wt}: The wild-type cell trait, i': The cheating mutant trait ($i_{wt} < i'$). $W(i';i_{wt})$: Invasion fitness of the cheating mutant within the wild-type population. t: development time with slug migration. $t = 0$: The slug stage, $t = 1$: the maximum migration time. Red lines indicate the analytical predictions of whether the cheater invades the wild-type population. The cheater can invade under the conditions below the red line in the canonical allocation system, and above the line in the reverse allocation system. In random allocation, cheating always evolved. Initial cell fate probability of the mutant being prespore: 0.8, prestalk: 0, solitary cell: 0.2, that of the wild-type strain being prespore: 0.6, prestalk: 0.2, solitary cell: 0.2 are shown.